GlueX Document
Written or last updated: January 27, 2007

Analysis of BCAL Test Runs 2334 and 2363

Alex R. Dzierba

Run Conditions and BCAL Sums This note summarizes results of a comparison of BCAL test run numbers 2334 and 2363. The data were collected in September 2006. For this particular run the photon beam was centered on the calorimeter module (horizontally and vertically) and directed at 90° for run 2334 and 40° for run 2363.

The data shown include only those events for which there is only one beam photon in the event and the TDC readout for this beam photon was required to lie in the range from 580 to 610 ns. Figure 1 shows the distribution of the sum of the 18 phototubes at the North end of the module and the corresponding sum at the South end for the two runs.

First-order calibration: Figure 2 shows the distribution of the ratio of the beam energy as measured by the tagger to the BCAL energy measurement (the geometric mean of the North counters and South counters sums) for the two runs. The mean of the distribution is our approximate calibration constant. The means for the normal and 40° incidence are 0.196 ± 0.002 and 0.189 ± 0.002 respectively. Figure 3 shows the distribution of beam energy as measured by the tagger (filled histogram) and the calibrated energy reported by BCAL run 2334 (normal incidence) and run 2363 (40° incidence).

Energy resolution: Figure 4 shows the resolution as a function of energy run 2334 (normal incidence) and run 2363 (40° incidence). The curves are a fit to a function of the form:

$$\frac{\sigma_E}{E} = \frac{a}{\sqrt{E(GeV)}} + b$$

For normal incidence $a = 0.0479 \pm 0.004$ and $b = 0.0228 \pm 0.007$ and for 40° incidence $a = 0.0497 \pm 0.003$ and $b = 0.0204 \pm 0.006$. As expected, the energy resolution should be independent of angle of incidence.

Please note that my calibration is approximate and the same constant applies to each phototube. When Blake Leverington allows the constants to vary for each tube but then requires that the width of the difference (between beam energy and BCAL energy) distribution be minimized, he obtains a smaller (by factor of two) floor term. The statistical term is about the same. Also, I observe that the mean of the difference distributions is constant with energy.

TDC information: I do not know to what extent the TDC information is calibrated, but to first order the TDC information looks rational. Figures 5 and 6 show the North – South time difference, Δt (ns), for the middle sector for the six layers (increasing layer number is in the beam direction) for the two runs. The means of these distributions – with error bars representing widths – are summarized in Figure 7. As expected, the width increases with increasing layer number and the mean is relatively constant for normal incidence and changes with layer number for 40° incidence. The time difference distributions for the top, middle and bottom sectors for the first layer for the two runs are shown in Figure 8. The beam is incident on the middle sector.

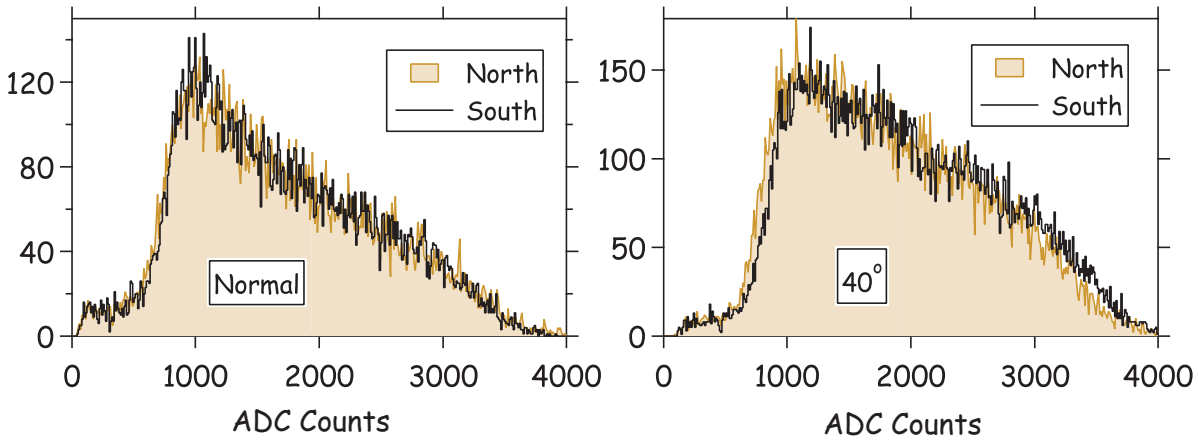

Figure 1: Distribution of the sum of the 18 phototubes at the North end of the BCAL module (filled histogram) and the corresponding sum for the South (unfilled histogram) end for run 2334 (normal incidence) and run 2363 (40° incidence).

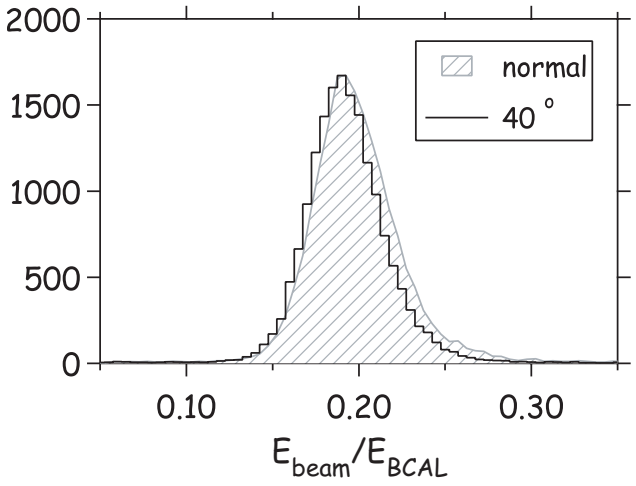

Figure 2: Distribution of the ratio of the beam energy as measured by the tagger to the BCAL energy measurement (the geometric mean of the North counters and South counters sums) for the two runs. The mean of the distribution is our approximate calibration constant. The means for the normal and 40° incidence are 0.196 ± 0.002 and 0.189 ± 0.002 respectively.

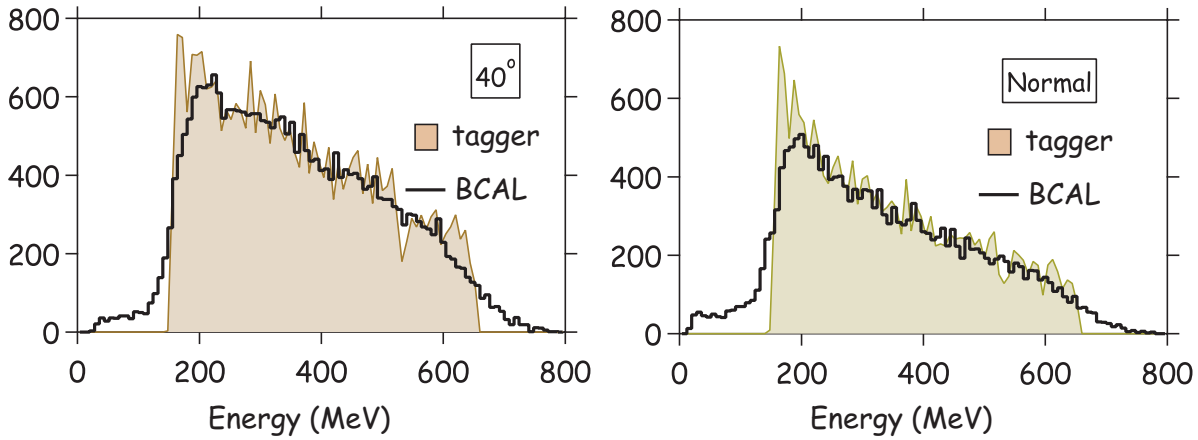

Figure 3: Distribution of beam energy as measured by the tagger (filled histogram) and the calibrated energy reported by BCAL run 2334 (normal incidence) and run 2363 (40° incidence).

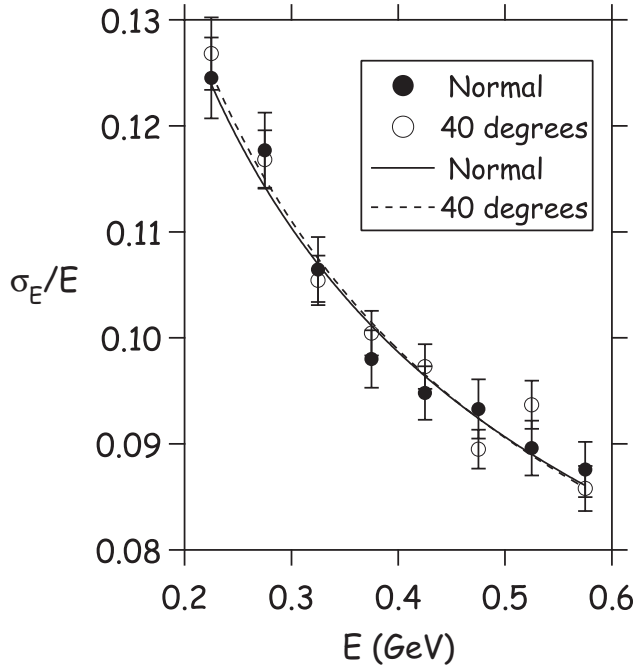

Figure 4: Resolution as a function of energy run 2334 (normal incidence) and run 2363 (40° incidence).

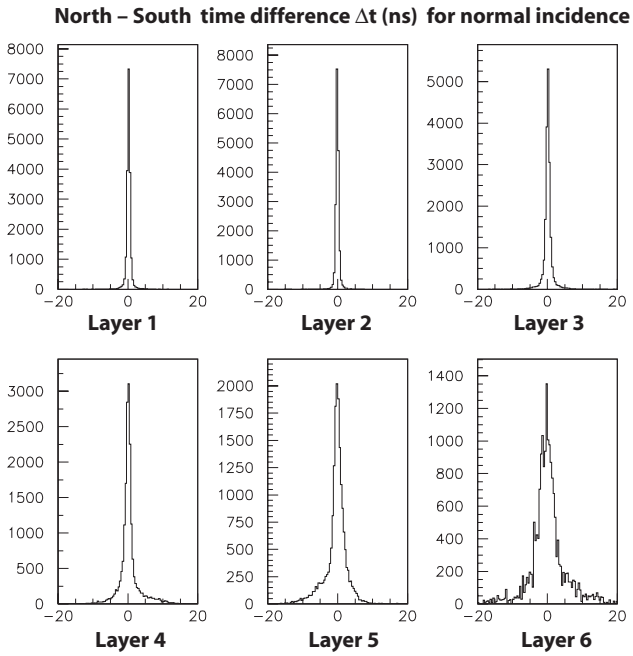

Figure 5: North – South time difference, Δt (ns), for the middle sector for the six layers for run 2334 (normal incidence).

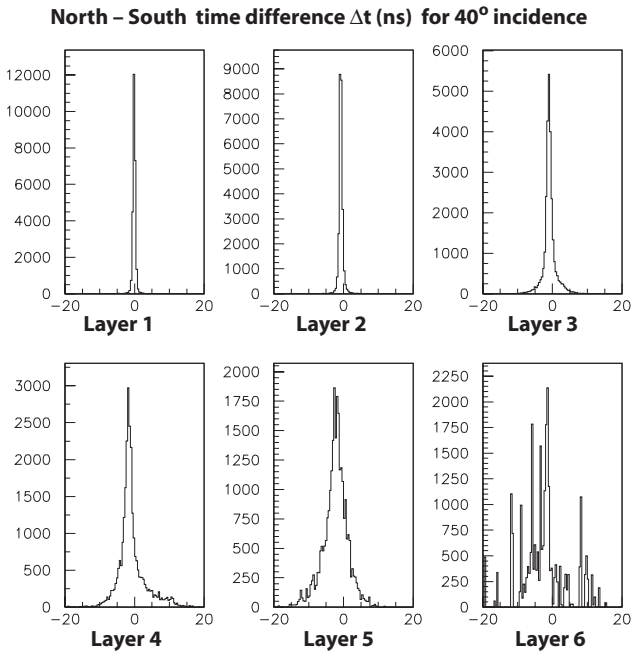

Figure 6: North – South time difference, Δt (ns), for the middle sector for the six layers for run 2363 (40° incidence).

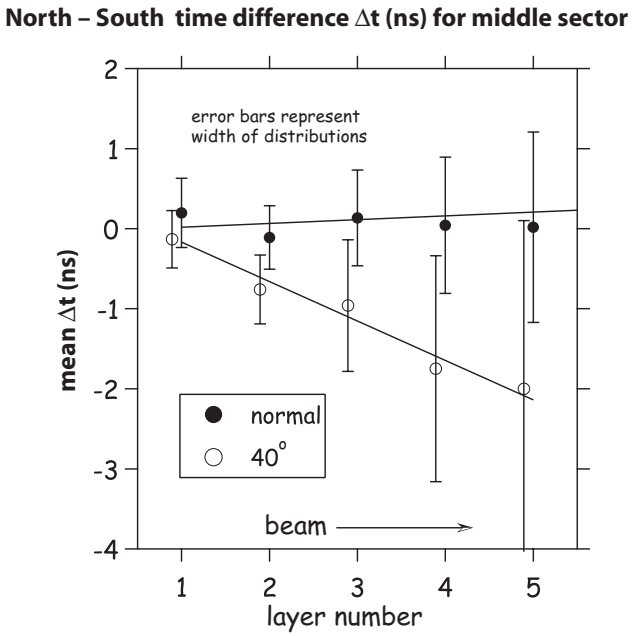

Figure 7: The means of the distributions shown in Figures 5 and 6 as a function of layer number. The error bars represent the widths of the distributions.

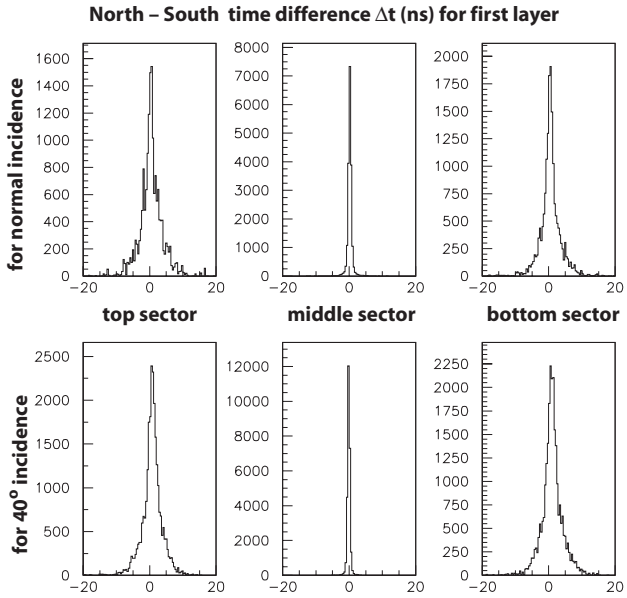

Figure 8: North – South time difference, Δt (ns), for the first layer for the top, middle and bottom sectors run 2334 (normal incidence) and run 2363 (40° incidence).